

Energy dependence of the valon-valon matter form factor

S. Sanielevici and P. Valin

Physics Department, McGill University, Montreal, Quebec, Canada H3A 2T8

(Received 4 December 1984)

Using the short-range-expansion formalism we simultaneously fit the pp elastic differential cross section (DCS) as $\sqrt{s} = 52.8$ GeV and the newest $\bar{p}p$ DCS data measured by UA4 at the CERN SPS $\bar{p}p$ collider (S $\bar{p}p$ S). This amounts to a prediction of the large- t behavior of the S $\bar{p}p$ S DCS. The corresponding valon-valon matter form factor has a zero at a smaller Q^2 than it has at $\sqrt{s} = 52.8$ GeV. We show that, as s increases from CERN ISR to S $\bar{p}p$ S and beyond, the valon, like its host hadron, becomes larger and blacker while still remaining about half the size of its host. A qualitative physical explanation of this behavior is suggested.

I. INTRODUCTION

In a previous paper,¹ we argued for the use of matter form factors (MFF's) as an arena of confrontation between theoretical descriptions of dynamic hadron structure, on one hand, and high-energy elastic hadron-hadron scattering data on the other hand. Specifically, we analyzed the pp and πp MFF's extracted from CERN ISR and Fermilab differential-cross-section (DCS) data in terms of the valon model discussed in Ref. 2.

Denoting the c.m. energy squared by s , the impact parameter by b , and the four-momentum transfer squared by $t = -Q^2$, we define the MFF corresponding to high- s $AB \rightarrow AB$ elastic scattering as the Fourier-Bessel transform of the eikonal $\Omega(s, b)$ (Ref. 3)

$$M_{AB}(s, t) = \int_0^\infty \Omega(s, b) J_0(b\sqrt{-t}) b db \quad (1)$$

and assume it can also be written as

$$M_{AB}(s, t) = K_A(Q^2) K_B(Q^2) V(s, Q^2). \quad (2)$$

Here K_A, K_B are due to the matter distributions of structureless valons in the colliding hadrons A, B , as determined in the valon-model analysis of high- Q^2 deep-inelastic lepton-hadron scattering.^{1,4} $V(s, t)$ is the universal valon-valon ("reduced") MFF (Ref. 1).

The most striking feature of the MFF's extracted from experimental data in Ref. 1 is that they all pass through zero beyond $Q^2 \cong 5$ GeV². This is intimately related to the behavior of the corresponding differential cross sections at such large values of $-t$, notably to the absence of further dips. By predicting the πp MFF at $p_{\text{lab}} = 200$ GeV/ c from the pp MFF at $\sqrt{s} = 52.8$ GeV we found that Eq. (2) gives good results modulo the s dependence of the zero in the (reduced) MFF (see Fig. 4 in Ref. 1). Given the universal features of MFF's that one could extract from DCS data up to the highest measured t values, we will again assume the validity of (2) for all measured t values of the DCS at the CERN SPS $\bar{p}p$ collider (S $\bar{p}p$ S). Since the relevant t range decreases experimentally as s increases due to the shrinkage of the forward peak, we expect our analysis to become increasingly more valid as s increases.

The idea of "equivalent energies" for different hadron-

hadron systems, at which the factorized ansatz (2) is exact,¹ is an expression of the following observation: let x_A, x_B be the longitudinal-momentum fractions of valons in hadrons A, B (in the coordinate system discussed in Ref. 5 and used in Ref. 1). Strictly speaking, V should be a function not of s , but $\hat{s} = x_A x_B s$, the fraction of the total c.m. energy which is available for valon-valon scattering. The factorized ansatz Eq. (2) can only be an approximation. We should properly write

$$M_{AB}(s, Q^2) = \int_0^1 dx_A \int_0^1 dx_B [K_A(x_A, Q^2) K_B(x_B, Q^2) \times V(\hat{s}, Q^2)], \quad (3)$$

but as long as we do not know the analytical form of $V(\hat{s}, t)$, we must use Eq. (2) to compare valon-model calculations to data, thereby testing its validity as an approximation to Eq. (3). To see that such a convolution leads to the concept of "equivalent energies" for different reactions, let us take the simplistic case of a factorizable $K_C(x_C, Q^2) = \delta(x_C - \bar{x}_C) K_C(Q^2)$ with different \bar{x}_C for different particles [e.g., $\frac{1}{2}$ for mesons ($C=M$) and $\frac{1}{3}$ for baryons ($C=B$)]. We then have

$$M_{MB}(s, t) = K_M(Q^2) K_B(Q^2) V(\bar{x}_M \bar{x}_B s, Q^2)$$

but

$$M_{BB}(s, t) = K_B^2(Q^2) V(\bar{x}_B^2 s, Q^2);$$

hence to obtain a unique expression for V one should compare the extracted $MB \rightarrow MB$ MFF at an s value \bar{x}_B / \bar{x}_M times the one for the $BB \rightarrow BB$ reaction.

The quality of the DCS data at the other ISR energies was not sufficient to enable us to extract a clear trend in the s evolution of experimental MFF's (see Fig. 1 of Ref. 1). The only way to look for a clear signal on the s dependence of the reduced MFF is to analyze the collider data. Note that, under the standard assumption of Pomeron dominance,⁶ the $\bar{p}p$ MFF should be identical to the pp MFF at the same (high) energy.

II. THE MFF FROM ISR TO S $\bar{p}p$ S

The UA4 collaboration has measured the $\bar{p}p$ total cross section⁷ at $\sqrt{s} = 546$ GeV to be 61.9 mb. Their elastic

DCS data^{8,9} are represented by solid dots in Fig. 1. In order to extract the corresponding MFF we use the following parametrization of the spin-nonflip, purely absorptive elastic scattering amplitude,¹ based on the latest UA4 fits⁹ to the measured DCS [in GeV^{-2} , with normalizations $d\sigma/dt = \pi |f(s,t)|^2$ and $\sigma_{\text{tot}} = 4\pi \text{Im}f(s,0)$, and t in GeV^2],

$$\text{Im}f(t) = \begin{cases} 12.65e^{7.6t}, & 0 \leq |t| \leq 0.15, \\ 11.376e^{7.1t}, & 0.15 \leq |t| \leq 0.21, \\ 10.79e^{6.7t}, & 0.21 \leq |t| \leq 0.5. \end{cases} \quad (4)$$

For $|t| \geq 0.5 \text{ GeV}^2$, we use¹⁰

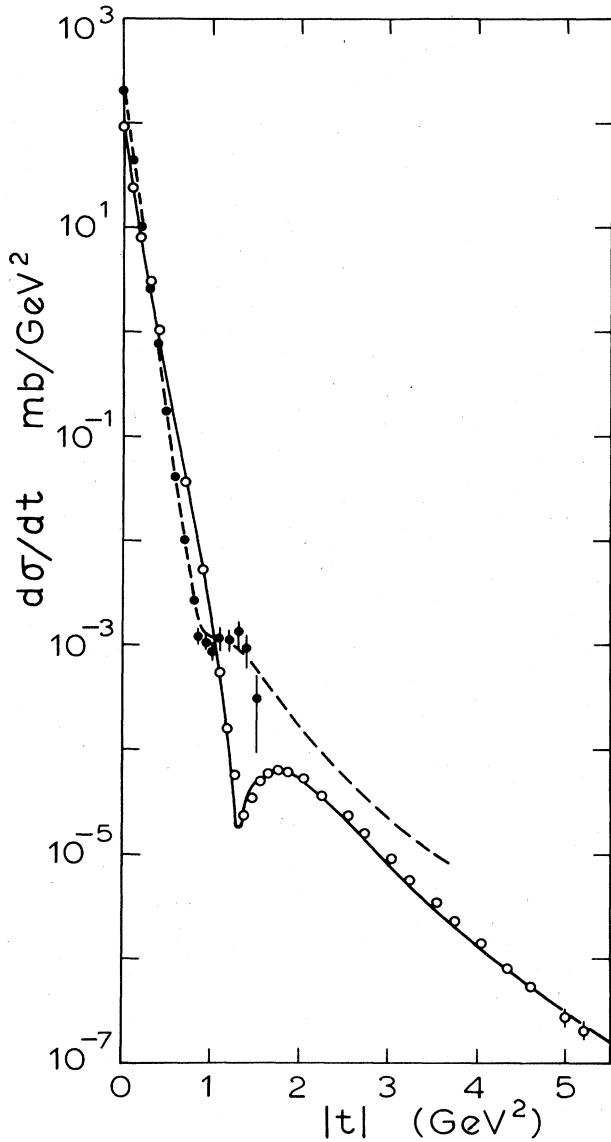


FIG. 1. Simultaneous SRE fit to the pp DCS at $\sqrt{s} = 52.8 \text{ GeV}$ and to the $\bar{p}p$ DCS at $\sqrt{s} = 546 \text{ GeV}$. ISR data are represented by open dots and UA4 data by solid dots. The solid curve is the fit to ISR data and the dashed curve is the fit to the UA4 data (up to $-t = 1.5 \text{ GeV}^2$). Beyond 1.5 GeV^2 the dashed curve is a prediction. Typical error bars are shown.

$$\text{Im}f(t) = \text{Re}[0.10725e^{i\theta}(e^{5.45(t-t_0)} + e^{i\phi+2.3(t-t_0)})], \quad (5)$$

with $-t_0 = 0.81 \text{ GeV}^2$, $\phi = \pi - 0.39$, and $\theta = 0.13$. As suggested by the UA4 group, we have used smoothly connected exponentials instead of the sum of exponentials used in Ref. 1. The elastic profile $h(s,b)$ is then obtained in the standard way as the Fourier-Bessel transform

$$h(s,b) = \int_0^\infty \text{Im}f(s,t) J_0(b\sqrt{-t}) \sqrt{-t} d\sqrt{-t}. \quad (6)$$

The corresponding eikonal

$$\Omega(s,b) = -\ln[1 - h(s,b)] \quad (7)$$

is then used to calculate the resulting $M_{\bar{p}p}(s,t)/M_{\bar{p}p}(s,0)$ which is represented by the dots in Fig. 2. Since the DCS has only been measured up to $|t| = 1.5 \text{ GeV}^2$, we cannot trust the corresponding MFF beyond roughly 1 GeV^2 .

To make a statement about the zero in the MFF at the collider energy we must thus predict the large- t DCS. We do this by performing a simultaneous fit to the measured $S\bar{p}pS$ DCS and to the DCS measured at the ISR energy of $\sqrt{s} = 52.8 \text{ GeV}$, using the short-range expansion (SRE) ansatz^{6,10,11} for the inelastic overlap function $G(s,b)$:

$$G(s,b) = P e^{-b^2/4B} \sum_{n=0}^2 \delta_{2n} \left[\frac{\gamma b}{\sqrt{2B}} e^{1/2 - (\gamma b)^2/4B} \right]^{2n}. \quad (8)$$

This is an expansion of the inelastic overlap function $G(s,b)$ around a Gaussian form, in terms of the short-range variable ($b e^{-(\gamma b)^2/4B}$) where the argument of the

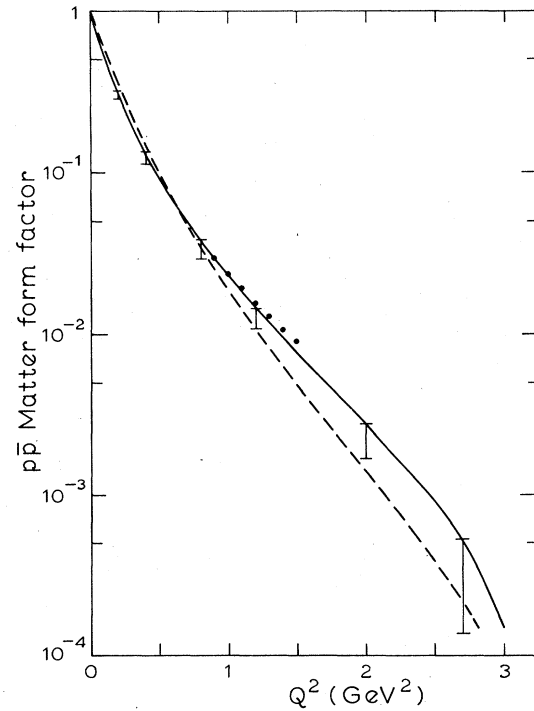


FIG. 2. Various $\bar{p}p$ MFF's at $\sqrt{s} = 546 \text{ GeV}$. These MFF's are normalized to unity at $t=0$. Dots represent the extraction from UA4 DCS data. The solid curve corresponds to the smallest value of the SRE parameter B compatible with the fit in Fig. 1. The error bars are induced by the errors listed in Table I. The dashed curve represents Eq. (15) with $a^2 = 3.2 \text{ GeV}^2$.

power series is chosen such that its maximal value be unity. Given the simplifying assumptions that γ is constant⁶ and $\delta_4 = \delta_2^2/4$ (Ref. 11), a simultaneous fit to the DCS data at two c.m. energies determines a well-defined evolution of each of the three remaining parameters with the increase of s . Setting $y = \ln^2(s/s_0)$ with $s_0 = 100 \text{ GeV}^2$ one writes

$$\begin{aligned} P(y) &= \frac{b+cy}{l+cy}, \\ B(y) &= d+ey, \\ \delta_2(y) &= f+gy, \end{aligned} \quad (9)$$

as discussed in the Bern talk of Ref. 6 and in the Syracuse talk of Ref. 10. The fit shown in Fig. 1 is obtained for the parameter values quoted in Table I.

The errors on the parameters in Eqs. (9) (see Table I) induce errors in the corresponding MFF. In Fig. 2 the solid curve corresponds to the lowest value of B ($\sqrt{s} = 546 \text{ GeV}$) compatible with the fit and the error bars show the effect of the uncertainty in the SRE parameters on the corresponding normalized MFF. We have represented this curve because it coincides with the extraction from Eqs. (4) and (5) up to $Q^2 \cong 1 \text{ GeV}^2$; for $Q^2 \gtrsim 1 \text{ GeV}^2$ it amounts to a prediction of the $\bar{p}p$ MFF, corresponding to the dashed curve in Fig. 1. Our predicted $S\bar{p}pS$ MFF has a zero at $a^2 \cong 3.2 \text{ GeV}^2$, whereas the pp MFF at $\sqrt{s} = 52.8 \text{ GeV}$ had its zero at $a^2 \cong 5.67 \text{ GeV}^2$.

We can obviously use Eqs. (8) and (9) to extract the pp ($\bar{p}p$) MFF at other energies as well. Figure 3(a) shows the corresponding s dependence of the quantity

$$f(s) = M_{pp}(s, 0) \quad (10)$$

and Fig. 3(b) displays the s evolution of the zero in the MFF. Error bars are again induced by the parameter uncertainties listed in Table I. Slightly larger error bars are obtained if we compare different versions¹⁰ of the SRE analysis: one which gives a detailed description of the ISR regime, and yet another one which is especially designed for the analysis at very high energies (the Superconducting Super Collider and beyond) since it explicitly satisfies unitarity at asymptotically large s . We find that this does not affect the conclusions we draw from Figs. 3(a) and 3(b), namely that $f(s)$ is very well described by

$$f(s) \sim s^\epsilon, \quad \epsilon \cong 0.105 \quad (11)$$

and that the zero in the (reduced) MFF decreases in a very specific way as s increases.

III. BEL AND THE VALON

Can we interpret these findings physically? The increase of the SRE parameters with s according to Eqs. (9) has a simple physical interpretation:^{6,10} the proton (an-

TABLE I. Parameters in Eq. (9) used for the fit shown in Fig. 1. d and e are in GeV^{-2} .

b	0.912 ± 0.004	c	0.026 ± 0.006
d	6.530 ± 0.211	e	0.045 ± 0.008
f	0.118 ± 0.0026	g	0.0009 ± 0.0001

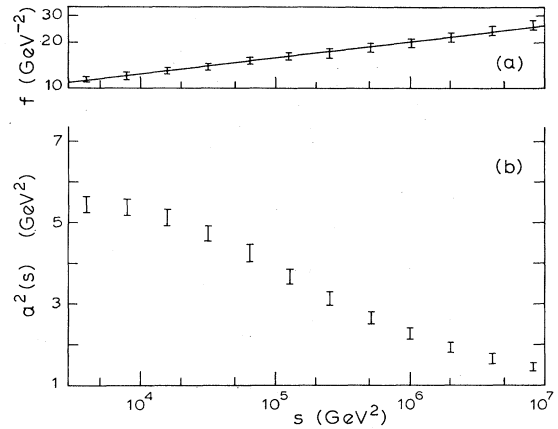


FIG. 3. (a) $f(s)$ and (b) $a^2(s)$ according to the SRE fit in Fig. 1. Error bars are induced by the errors listed in Table I. The straight line in (a) corresponds to $\epsilon = 0.105$ in Eq. (11) [or (16)].

tiproton) becomes blacker as P increases, larger as B increases, and edgier (that is, closer to having a step-function profile) with the increase of δ_2 . The valon model interpretation of MFF's allows us to trace this so-called "BEL" behavior to the (as yet) qualitative dynamics of valon-valon scattering.

In Ref. 12 we linked the phenomenological valon model to a simple two-scale picture of hadron structure suggested by nonperturbative dynamical mechanisms for chiral-symmetry breaking and confinement in QCD. Dynamical quark mass generation in QCD implies that the valon ("constituent quark") is identical to the chiral-symmetry-breaking color-field ("parton") configuration G_χ , which is characterized by a fundamental scale parameter Λ_χ . Confinement can be described as dynamical gluon mass generation, expressing the existence of a color field configuration G_c with the fundamental scale $\Lambda_c \cong 200 \text{ MeV}$. The two scale parameters must satisfy the inequality

$$\Lambda_\chi \geq \Lambda_c. \quad (12)$$

The valon model is a phenomenological implementation of the two-scale idea. Consider lepton-hadron scattering as an "electroweak gauge boson microscope" with resolution Q^2 (see Ref. 12). For $Q^2 \lesssim 10 \text{ GeV}^2$ (Ref. 5), the impulse approximation for the interaction of the virtual photon (or W, Z) with the probed constituent allows one to factor off confinement dynamics into distributions of valons in the host hadron. The distribution of partons in a valon is then independent of the confinement problem. This universal distribution, independent of flavor and host hadron, is generated by chiral-symmetry breaking and is therefore governed, to a first approximation,¹² by a single parameter Q_0^2 which expresses the existence of Λ_χ . Valon structure is not resolved at resolution scales below Q_0^2 . At the same time, Q_0^2 also sets the scale of the spatial size of a valon.

Analogously, let us consider hadron-hadron (HH) scattering as a "gluon microscope." Now we have two resolution variables s and t . As opposed to t , s explores the on-shell dynamics of hadronic matter, the dynamical

excitations of hadronic substructure. Pumping large amounts of s into hadrons may cause G_c and then G_χ to break apart, thereby producing QCD plasma in the laboratory. It is generally agreed that it will take high-energy heavy-ion collisions to realize this possibility, which thus remains experimentally off-limits for HH scattering. We shall therefore restrict ourselves to the hypothesis that dynamical excitations produced in such collisions cannot break up the bound-state structure of valons and hadrons. This motivates the ansatz for $M_{AB}(s,t)$ given in Eq. (2). According to the static two-scale picture, the K 's embody the binding of valons into hadrons; since deconfinement of valons is not supposed to occur, K_A and K_B must be s independent. All the s dependence of M must be contained in the reduced MFF. $V(s,t)$ must have the general form

$$V(s,t) = f(s)W(s,t). \quad (13)$$

In Ref. 1 we used a simple ansatz for the reduced MFF (normalized to one at $Q^2=0$)

$$W(s, Q^2) = \frac{a^2(s) - Q^2}{a^2(s) + Q^2}. \quad (14)$$

It continues to be a fair first approximation at the $S\bar{p}pS$: the dashed curve in Fig. 2 is obtained by fixing the parameter a^2 in the formula

$$M_{\bar{p}p}(s, Q^2)/M_{\bar{p}p}(s, 0) = K_p^2(Q^2) \frac{a^2(s) - Q^2}{a^2(s) + Q^2} \quad (15)$$

to the SRE-predicted value of 3.2 GeV². Let us therefore use Eq. (14) in our heuristic discussion of the valon-valon MFF.

In the denominator of the effective expression (14), the timelike pole a^2 is seen to govern the size of the parton distribution in the overlapping valon-valon system at a given s . In this sense, it generalizes the scale Q_0^2 . The zero in the numerator indicates that for $Q^2 \geq a^2$ valons no longer scatter as structureless objects. Indeed, in the Chou-Yang droplet model, an infinite number of structureless, infinitely small scatterers leads to a t -independent MFF (since the Fourier transform of a δ function is a constant). For this range of Q^2 , we therefore deduce that complicated processes involving constituents of valons set on. This is again in agreement with the idea that a^2 generalizes Q_0^2 .

The s dependence of a^2 means the existence of a functional relationship between s and Q^2 ["scaling" of W in $Q^2/a^2(s)$]. The decrease of a^2 with s is then intuitively understandable: as s increases the structure inside valons becomes manifest "sooner" at smaller $-t$. Since a^2 also governs the size of the parton distribution, we see that valons (and hence hadrons) become larger as s increases.

At this point, one may wonder about the relative sizes of the valon V and its host hadron H and the ensuing usefulness of a decomposition such as the one in Eq. (2). If the relative positions of the single zeros of the HH amplitude [called $-t_0(s)$] and the VV amplitude [which is $a^2(s)$ of the MFF] are an indication of the relative sizes of these objects, then the radii are in the ratio

$$R_V/R_H = [-t_0(s)/a^2(s)]^{1/2}.$$

At both the ISR and the $S\bar{p}pS$ this ratio is approximately $\frac{1}{2}$, i.e., the valon's size is always roughly half that of the proton. We conclude that Eq. (2) remains useful for the whole energy range studied and that valons, like their host hadrons, become larger as s increases, in the ratio $R^2(\sqrt{s}=546)/R^2(\sqrt{s}=53) \cong 1.7$, which is not too far from what one would expect from studying the increase of $\sigma_{\text{tot}}^{pp}(s)$. If one uses the forward slopes of the amplitudes as an indication of the relative sizes, our conclusions would qualitatively be the same.

Let us now note that one can only define the average color and the average spin projection of a valon, since these quantities perpetually fluctuate due to random emission and absorption of infrared soft gluons.¹³ As in QED, there must be an infinite cloud of such wee gluons surrounding any partonic Fock state, that is, all valons at all stages of their Q^2 evolution. It has been known for a long time¹⁴ that "wee," soft gluons contribute significantly to the rise of the total HH cross section with s . It is thus natural to associate the Q^2 -independent factor $f(s)$ in Eq. (13) with the "blackening" of the infrared soft gluon clouds as s increases. It is interesting to note that the presence of a factor of the form

$$f(s) \sim s^\epsilon \quad (16)$$

has long ago been argued¹⁵ to be a general consequence of field-theoretic models with soft infrared quanta and it underlies the s dependence of factorizable eikonal (FE) type geometrical models of high-energy elastic hadron-hadron scattering. The value of ϵ has not been theoretically calculated for QCD. In fact, as in all problems involving infrared soft quanta, one can only expect an effective parametrization obtained by fitting Eq. (16) to experimental data. Our Fig. 3(a) shows that Eq. (16) is a remarkably good approximation over a wide range of s ; our value for ϵ is consistent with the estimates of Refs. 15 and 16.

We have inferred that the colliding valon-valon system becomes larger and "blackier" with increasing s . Equation (13) shows that it does so in a manner which is reminiscent of FE models [the factor $f(s)$] but which also has "scaling" effects built into it through the s dependence of the zero in the reduced MFF. These are precisely the qualitative features of BEL behavior. It is an intriguing task for the future to prove that valon-valon scattering actually is the underlying dynamics of BEL behavior, by deriving the motion of the zero from nonperturbative QCD. Should one be able to find a parametrization for $a^2(\hat{s})$, one might try to represent $V(\hat{s}, t)$ by Eqs. (13) and (14) and then use it in Eq. (3). One could then calculate $G(s, b)$ from $M(s, t)$ and would hopefully reproduce the SRE analysis.

The question arises whether a^2 is really constant at low s (in the ISR regime and below). We performed an SRE extraction of the pp MFF at $p_{\text{lab}}=400$ GeV/ c and found the zero at $\cong 6.02$ GeV². Together with our observation in Ref. 1 that the πp MFF at $p_{\text{lab}}=200$ GeV/ c has its zero at $a^2 \cong 8.5$ GeV², this indicates that $da^2/ds < 0$ also at lower energies. It seems however that, in this region, the relevance of the motion of the MFF zero for the DCS is overshadowed by Regge effects.

IV. DISCUSSION

We have used SRE parametrizations to display the energy dependence of reduced MFF's as s varies from ISR to $S\bar{p}pS$ and beyond. We relate the characteristic BEL behavior of such parametrizations to the nonperturbative dynamics of valon-valon scattering.

The SRE formalism gives an excellent simultaneous description of all elastic scattering observables at ISR and $S\bar{p}pS$.^{6,10,11} It improves upon the performance of both geometrical-scaling (GS) and FE models, whose s dependences can be viewed as too restrictive particular cases of BEL behavior. Indeed, GS hadrons only become larger as s increases, while FE hadrons become excessively black at the expense of an insufficient size increase which causes too small an increase of the forward logarithmic slope of the DCS as a function of s . Some FE models¹⁷ have actually had to become edgier and larger to improve their performance.

We have found that the Fourier-Bessel transform of the eikonal is well approximated by the generic form

$$M_{AB}(s,t) = F_{AB}(t)f(s)W(s,t), \quad (17)$$

where $F_{AB}(t)$ is related to the convolution of matter distributions in the colliding hadrons, $f(s)$ is of the form (16) and $W(s,t)$ features a zero at a value of Q^2 which decreases as s grows. Other geometric models of high-energy elastic hadron-hadron scattering can be viewed as particular cases of Eq. (17).

The new "edgy" version of the Chou-Yang model parametrizes the eikonal as¹⁷

$$\Omega(s,b) = A(s) \left[\frac{s}{s_0} \right]^{Cb} \Omega_0(b) \quad (18)$$

which, upon Fourier-Bessel transformation, will yield an expression of the form (17).

Chiu¹⁸ writes

$$M(s,t) = iK(Ee^{-i\pi/2})^C \exp\{-B[(\lambda^2 - t)^{1/2} - \lambda]\}, \quad (19)$$

$$B = b_0 + b_1[\ln(E/E_1) - i\pi/2], \quad E_1 = 1400 \text{ GeV}$$

with $E = s/2m_p$. His parametrization of $W(s,t)$ does not have a zero because it does not apply for $|t| \geq 1.2 \text{ GeV}^2$.

Glauber and Velasco¹⁹ analyze the small- t $S\bar{p}pS$ DCS

data using

$$M_{\bar{p}p}(t)/M_{\bar{p}p}(0) = G_p^2 \Phi(t) \quad (20)$$

with G_p given by parametrizations which successfully describe the proton electric form factor as probed in electron-proton scattering. A future extension of their model to variable s and to large $|t|$ would presumably also lead to the general form (17). Indeed, if we too restrict our analysis to small- $(-t)$ data, we see that, since our $a^2(s)$ increases from $S\bar{p}pS$ to ISR, their equivalent parameter in $\Phi(t)$ has to follow suit, a fact which these authors preliminarily report. Note that their multiple scattering analysis lends support to the idea that the factorized ansatz (2) [or (17)] is exact at fixed s , for a given reaction.

On the other hand, Bourrely, Soffer, and Wu (BSW) still use a purely FE-type ansatz^{16,20}

$$M(s,t) = \frac{1}{(1-t/m_1^2)(1-t/m_2^2)^2} S_0(s) \frac{a^2+t}{a^2-t}. \quad (21)$$

The presence of the zero enables them to analyze the large- t but its lack of s dependence leads to the aforementioned, generic FE problem with the forward logarithmic slope. However, it is interesting to note that the simultaneous BSW fit to ISR and $S\bar{p}pS$ data reported in Ref. 16 requires $a^2 \cong 3.8 \text{ GeV}^2$, whereas their previous fit to ISR data alone²⁰ required $a^2 \cong 5.1 \text{ GeV}^2$.

Our model thus combines the data-reproducing features of other approaches while reducing the number of parameters and offering a simple interpretation of the observed behavior in terms of popular ideas about nonperturbative QCD. It also offers the hope of going beyond the factorized approximation (17). Its value depends, of course, on the quality of its predictions about large- t elastic scattering at the $S\bar{p}pS$ and about the MFF at other values of s , as well as on the ultimate calculability of its parameters from nonperturbative QCD.

ACKNOWLEDGMENTS

We would like to thank R. Henzi for useful discussions. This work was supported in part by the Natural Sciences and Engineering Research Council of Canada and by the Québec Department of Education.

¹S. Sanielevici and P. Valin, Phys. Rev. D **29**, 52 (1984).

²R. C. Hwa, in *Partons in Soft Hadronic Processes*, edited by R. T. Van de Walle (World Scientific, Singapore, 1981); University of Oregon Institute for Theoretical Science Report No. OITS 206, 1983 (unpublished).

³In Ref. 1 we normalized MFF's to 1 at $t=0$. This is natural when s is fixed and we plot normalized MFF's in Fig. 2 of this paper. For the purpose of studying the s dependence we prefer, however, to define the MFF as in Eq. (1), since factors which depend only on s cancel out upon normalization. With this definition, MFF's have dimensions of scattering amplitudes. Normalized MFF's are dimensionless.

⁴R. C. Hwa and M. S. Zahir, Phys. Rev. D **23**, 2539 (1981); **25**,

2455 (1982).

⁵R. C. Hwa and C. S. Lam, Phys. Rev. D **26**, 2338 (1982).

⁶R. Henzi and P. Valin, Phys. Lett. **132B**, 443 (1983); **149B**, 239 (1984); R. Henzi, in *Proceedings of the 4th Topical Workshop on Proton-Antiproton Collider Physics, Bern, 1984*, edited by H. Hanni and J. Schecher (Report No. CERN-84-09, 1984), pp. 314-321.

⁷M. Bozzo *et al.*, Phys. Lett. **147B**, 392 (1984).

⁸F. Cervelli, in *Proceedings of the 4th Topical Workshop on Proton-Antiproton Collider Physics, Bern, 1984* (Ref. 6).

⁹M. Bozzo *et al.*, Phys. Lett. **147B**, 385 (1984).

¹⁰P. Valin, Z. Phys. C **25**, 259 (1984); in *Proceedings of the 6th Montreal-Rochester-Syracuse-Toronto High Energy Theory*

- Meeting, Syracuse, 1984*, pp. 68–92.
- ¹¹R. Henzi and P. Valin, Nucl. Phys. **B148**, 513 (1979); Z. Phys. C **27**, 351 (1985).
- ¹²M. Nicolescu, S. Sanielevici, and P. Valin, McGill report (unpublished).
- ¹³R. C. Hwa and M. S. Zahir, Z. Phys. C **20**, 27 (1983).
- ¹⁴L. Van Hove, Acta Phys. Pol. B **7**, 339 (1976); Nucl. Phys. **B122**, 525 (1977); H. I. Miettinen and J. Pumplin, Phys. Rev. D **18**, 1696 (1978).
- ¹⁵H. Cheng and T. T. Wu, Phys. Rev. Lett. **24**, 1456 (1970); H. Cheng, J. K. Walker, and T. T. Wu, Phys. Lett. **44B**, 97 (1973).
- ¹⁶C. Bourrely, J. Soffer, and T. T. Wu, Nucl. Phys. **B247**, 15 (1984).
- ¹⁷T. T. Chou and C. N. Yang, Phys. Lett. **128B**, 457 (1983).
- ¹⁸C. Chiu, Phys. Lett. **142B**, 309 (1984).
- ¹⁹R. J. Glauber and J. Velasco, Phys. Lett. **147B**, 380 (1984).
- ²⁰C. Bourrely, J. Soffer, and T. T. Wu, Phys. Rev. D **19**, 3249 (1979).